

Wanyu R. Chan^{1,2*}, Phillip N. Price², Ashok J. Gadgil², William W. Nazaroff^{1,2},
Gwen Loosmore³, and Gayle Sugiyama³

¹University of California Berkeley, California

²Lawrence Berkeley National Laboratory, Berkeley, California

³Lawrence Livermore National Laboratory, Livermore, California

ABSTRACT

Intentional or accidental large-scale airborne toxic releases (e.g. terrorist attacks or industrial accidents) can cause severe harm to nearby communities. As part of an emergency response plan, shelter-in-place (SIP) can be an effective response option, especially when evacuation is infeasible. Reasonably tight building envelopes provide some protection against exposure to peak concentrations when toxic release passes over an area. They also provide some protection in terms of cumulative exposure, if SIP is terminated promptly after the outdoor plume has passed.

The purpose of this work is to quantify the level of protection offered by existing houses, and the importance of sorption/desorption to and from surfaces on the effectiveness of SIP. We examined a hypothetical chlorine gas release scenario simulated by the National Atmospheric Release Advisory Center (NARAC). We used a standard infiltration model to calculate the distribution of time dependent infiltration rates within each census tract. Large variation in the air tightness of dwellings makes some houses more protective than others. Considering only the median air tightness, model results showed that if sheltered indoors, the total population intake of non-sorbing toxic gas is only 50% of the outdoor level 4 hours from the start of the release. Based on a sorption/desorption model by Karlsson and Huber (1996), we calculated that the sorption process would further lower the total intake of the population by an additional 50%. The potential benefit of SIP can be considerably higher if the comparison is made in terms of health effects because of the non-linear acute effect dose-response curve of many chemical warfare agents and toxic industrial substances.

Keywords: Shelter-in-place, Infiltration, Sorption

1. INTRODUCTION

Intentional or accidental large scale outdoor airborne releases can cause severe harm to nearby communities. Conventional emergency planning has focused on deriving planning zones based on the distance from the hazardous source. The zone-maps are then used to guide preparations and training efforts. However, in the event of an atmospheric release, the particular situation might not be properly described by the zone-maps, which are developed by averaging over a number of possible scenarios. Models specific to release site and local meteorology would be valuable in predicting consequences of specific events.

For model prediction to be informative for emergency response, it must enable comparisons of the consequences of selecting evacuation versus shelter-in-place responses. Evacuation is effective if there is sufficient time for relocation. Transportation models can predict the amount of time required and determine if evacuation is a viable option. However, evacuation is both costly and logistically demanding. Also, if the weather pattern changes, there also lies the risk of exposing the evacuating population to the contaminant.

On the other hand, shelter-in-place can be effective even with little advance notice. A recent paper by Mannan and Kilpatrick (2000) listed some successful examples of shelter-in-place where injuries and fatalities were prevented. However, the authors also pointed out that many are skeptical of this form of protective action. Critics often challenge the reliability of shelter-in-place, and note the lack of experimental studies on its effectiveness.

* *Corresponding author:* Wanyu R. Chan,
Lawrence Berkeley National Laboratory,
Indoor Environment Department,
1 Cyclotron Road, Mailstop 90R3058,
Berkeley, CA 94720; email: wchan@lbl.gov

There have been a few experimental studies on the efficiency of some components of shelter-in-place, such as passive and active filtering (Blewett and Arca, 1999), duct tape and plastic sheets (Sorensen and Vogt, 2001), and the effect of turning on a shower (Blewett et al., 1996). However, the inherently large variations in air tightness of buildings have not been captured in past SIP modeling. A study by Vogt et al. (1999) mapped the age of the housing stock and used it as an indicator of the protectiveness of the dwellings. In this paper, we summarize the air leakage distribution of the housing stock, and then model the indoor concentration of both chemically inert and sorbing contaminants.

2. BACKGROUND

2.1 LBL Infiltration Model

When sheltering-in-place, doors and windows should be closed, and mechanical ventilation devices should be off. In such cases, air exchange occurs mainly by uncontrolled air leakage across the building envelope, a process known as air infiltration. Air infiltration is a function of the leakiness of the building and the differential pressures across the envelope, which are caused by indoor-outdoor temperature difference and the dynamic forces exerted by wind. The LBL infiltration model (Sherman, 1980) describes airflow Q_f [m^3/s] as follows:

$$Q_f = ELA \cdot \sqrt{f_s^2 \cdot |\Delta T| + f_w^2 \cdot v^2} \quad (1)$$

where ELA [m^2] is the effective leakage area of the building, $|\Delta T|$ [K] is the absolute indoor-outdoor temperature difference, and v [m/s] is the wind speed. The parameters f_s and f_w are known as the stack and wind factors, respectively.

The stack factor is a function of the air leakage distribution of the building envelope, as well as the height at which the pressure inside the building equals the pressure outside. Sherman (1980) expressed f_s as follows:

$$f_s = \left(\frac{1+R/2}{3} \right) \left(1 - \frac{X^2}{(2-R)^2} \right)^{3/2} \left(\frac{g \cdot H}{T_o} \right)^{1/2} \quad (2)$$

where R is the *sum* of the fractional air leakage in the floor and the ceiling, X is the fractional *difference* between the air leakage in the floor and the ceiling, H [m] is the height of the building, T_o [K] is the indoor temperature, and g is the gravitational acceleration. R and X are often assumed to be 0.5 and 0 respectively.

The wind factor accounts for the fact that the pressure exerted on the building envelope is less than what would occur for the wind speed measured at an elevated height. This is because of the height-dependent wind profile, but also because the building is often shielded from wind due to surrounding structures and objects. The wind factor may be estimated from this expression:

$$f_w = C \cdot (1-R)^{1/3} \cdot \frac{A \left(\frac{H}{10[m]} \right)^B}{A' \left(\frac{H'}{10[m]} \right)^{B'}} \quad (3)$$

where A and B are the terrain parameters at the building, A' and B' are the terrain parameters at the wind measurement site, C is the shielding parameter of the building, and R is the same as in Eqn. (2). H [m] is the height of the building, and H' [m] is the height at which the wind measurements are taken. Tables of the terrain and shielding parameters are presented in the Appendix.

2.2 Sorption-Desorption Model

For a conserved (non-reactive and non-sorbing) contaminant, the benefit of sheltering indoors is to reduce the peak concentration. Reasonably air tight houses restrict the rate at which the contaminant enters the indoor. As a result, the indoor concentration only rises to a fraction of the concentration outdoor. However, limited air exchange also means it will take a much longer time for the contaminant to exfiltrate. The exposure duration of the occupants to the contaminant is therefore extended. This change in exposure characteristics is desirable because of the non-linear acute effect dose-response curve of many toxic industrial substances and chemical warfare agents.

If air exchange rate remains constant, the total exposure indoor will approach the exposure outdoor with time. This is the case if SIP were allowed to continue long after the outdoor plume has passed. However, it is possible to increase the air exchange rate to facilitate decontamination by simple measures such as opening of doors and windows, and turning on mechanical ventilation. In such cases, the total exposure indoor can be reduced significantly.

The discussion above applies to non-reactive, non-sorbing contaminants. However, many contaminants of concern are fairly reactive, and for these, sheltering indoors has the advantage that some contaminants will be removed by two mechanisms: (1) when the contaminant first infiltrates the building envelope, some fraction of the contaminant may be lost from the air stream owing to filtering by the building materials; and (2) of the remaining fraction that enters indoor air, some may sorb to or react on indoor surfaces. These processes work together to further lower the indoor concentration of a reactive contaminant and provide another level of protection.

There have been a few studies on the indoor transformation processes of toxic industrial chemicals as well as some chemical warfare agents. Blewett and Arca (1999) studied the effect of passive and active filtering on the indoor concentration of sarin and mustard gases measured in a test cottage. Passive filtering, involving both filtration by building envelopes and sorption to indoor surfaces, was shown to greatly increase the protection factors of sheltering-in-place.

Karlsson and Huber (1996) formulated a simple two-parameter model to characterize the sorption/desorption process. In that paper, available data on sorption/desorption parameters are summarized for sarin, VX surrogate, NH_3 and Cl_2 .

Following the approach of Karlsson and Huber, the governing equation of the contaminant concentration indoors, C [mg/m^3], in a well-mixed room can be written as follows:

$$\frac{d(CV)}{dt} = Q_f \cdot C_{out} - Q_f \cdot C - \sum_i^N A_i \cdot \frac{dm_i}{dt} \quad (4)$$

where V [m^3] is the volume of the room, Q_f [m^3/s] is the infiltration rate, C_{out} [mg/m^3] is the outdoor concentration, N is the number of different materials, A_i [m^2] is the surface area of material i , and m_i [mg/m^2] is the net mass of contaminant taken up or reacted per unit area of material i . Karlsson and Huber (1996) also included a term to account for the presence of an internal filter, e.g., mask filters, lungs or other filtration equipment, which is not shown in Eqn. (4). Considering the case of reversible sorption, the rate of contaminant uptake, dm_i/dt [$\text{mg}/\text{m}^2 \cdot \text{s}$], on indoor surfaces is assumed to be proportional to the difference between the contaminant concentration in the air, C , and the concentration C_i^* in equilibrium with the deposited toxic gas on the surface material i .

$$\frac{dm_i}{dt} = a_i \cdot (C - C_i^*) \quad (5)$$

where a_i [m/s] is known as the transfer velocity. Transfer velocity depends on turbulent diffusion in the room, molecular diffusion in the viscous sub-layer, and characteristics of the indoor surface. According to the Langmuir theory (Nazaroff and Alvarez-Cohen, 2001), m_i is proportional to C_i^* for a given temperature at low vapor pressure:

$$C_i^* = b_i \cdot m_i \quad (6)$$

where b_i [m^{-1}] is an equilibrium parameter depending on gas properties, absorbing material, ambient temperature, and relative humidity. For high partial pressures, m_i is expected to approach a limiting value.

3. CASE STUDY

3.1 Hypothetical Release Scenario

The National Atmospheric Release Advisory Center (NARAC) at Lawrence Livermore National Laboratory performed a computer simulation of a hypothetical 4-hour chlorine gas release near downtown Albuquerque, New Mexico. The outdoor concentration predictions were generated from an atmospheric dispersion model known as the Lagrangian Operation Dispersion Integrator (LODI). The model solves the 3-D advection-diffusion equation using a Lagrangian stochastic, Monte Carlo approach. The model domain is 37 x 37 [km] at a grid

resolution that varies with the distance from source. The simulation used meteorological input dated February 24, 2003 from 18:00 to 22:00 hours.

LODI is capable of simulating first-order chemical reactions, among other atmospheric transformation processes. Since the simulation was during evening hours when there was no direct sunlight, we assumed that Cl_2 photolysis was not important and ignored the reactivity of Cl_2 in outdoor predictions. The outdoor concentration maps are displayed at 1, 2, 3, and 4 hours from the start of the simulation (see Appendix, Fig. (4)).

3.2 Air Leakage Distribution

Chan et al. (2003) analyzed blower-door test data from 70,000 residential houses in the US and characterized house leakage distribution as functions of house age, size, and household income. Instead of the effective leakage area as shown in Eqn. (1), the analysis was based on normalized leakage (NL), which is a leakage area normalized by the building floor area A_f [m^2] and incorporating a correction factor for the building height H [m].

$$NL = 1000 \cdot \frac{ELA}{A_f} \cdot \left(\frac{H}{2.5[\text{m}]} \right)^{0.3} \quad (7)$$

Normalized leakage is the preferred metric over ELA because it helps to describe the relative leakage for a wider range of building sizes. Using Eqn. (7), air infiltration rate Q_f [m^3/s] in Eqn. (1) can be expressed in terms of NL.

Analyses showed that the distribution of normalized leakage is approximately lognormal. Year built and floor area are the two most significant factors to consider when predicting air leakage distributions: older and smaller houses tend to have higher normalized leakage areas as compared to newer and larger ones. Results from multiple linear regression of normalized leakage suggested this relationship:

$$NL = e^{\beta_0 + \beta_1 \cdot \text{YearBuilt} + \beta_2 \cdot \text{Area} + \varepsilon} \quad (8)$$

where β_0 , β_1 , and β_2 are the regression parameters (see Appendix, Table 3). This relationship is only valid for detached, single-

family houses. Apartments and commercial buildings may have very different air leakage characteristics that are not described by this model. Also, Eqn. (8) predicts the *distribution* of air leakage for a housing stock, and *not* the leakage of a particular house. The form of a distribution can be obtained from the residual term, ε , which is normally distributed with $\mu=0.00$ and $\sigma^2=0.27$.

Inputs to Eqn. (8) include the structure year built, floor area and household income of the residential housing stock in Albuquerque. These data were obtained from the Census survey and American Housing survey conducted by the US Census Bureau. Detailed manipulations of these datasets are not discussed here, but the resulting distribution of normalized leakage of the housing stock in Albuquerque is shown in Fig. (1).

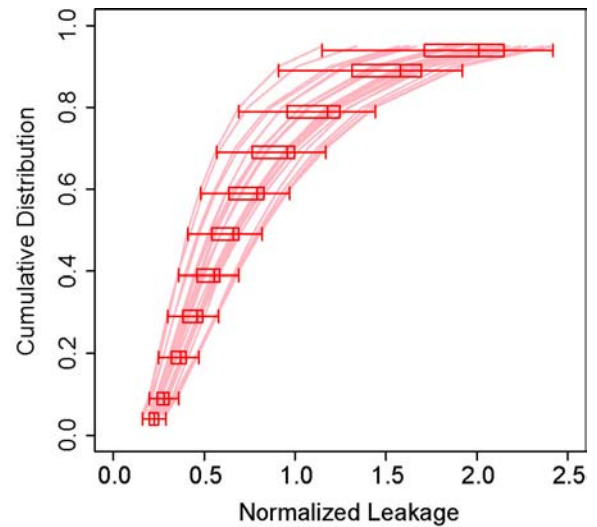


Fig. (1) Cumulative distributions of the normalized leakage of houses in 26 census tracts in Albuquerque exposed to the simulated Cl_2 plume. The box-plots show the median and inter-quartiles of normalized leakage of the houses.

Each cumulative distribution curve represents the normalized leakage distribution of houses in a census tract. In this particular release, the Cl_2 gas passed through 26 census tracts*. The box-

* Census tracts are small geographic subdivisions of a county. The number of people living in a census tract ranges from 1,000 to 8,000. Census tract boundaries

plots plotted on top of the individual cumulative distribution curves highlight the median and inter-quartiles of normalized leakage of the houses. There are considerable variations within and between census tracts in the leakiness of the houses from the different census tracts. The ratio of air tightness of the 95th to 5th percentiles of dwellings within a census tract falls between 7 to 10. The variation between census tracts is about a factor of 2.

3.3 Model Description

Under the instantaneous well-mixed assumption, houses can be modeled by a 1-box model. Eqn. (4), (5) and (6) are used to model the time-varying indoor concentration at each grid cell. At constant C_{out} and Q_f , an analytical solution can be obtained. However, both C_{out} and Q_f vary non-linearly with time, which requires a numerical method to predict indoor concentrations. We made the assumption that within a short time (1 minute), C_{out} and Q_f stay constant. The system of equations can then be solved analytically for each time increment, and the values for C_{out} and Q_f are updated after each 1-minute time step.

The outdoor concentrations C_{out} are the direct outputs from LODI at 15-minute intervals for the duration of the 4-hour release. Linear interpolation is used to estimate changes in C_{out} within the 15-minute interval. Similarly, linear interpolation is used to estimate the wind speed needed to calculate Q_f . The time-varying outdoor temperature profile is obtained from a weather station located in Albuquerque and is assumed to represent the temperature for the entire model domain. Indoor temperature is assumed to be a constant at 20 °C for all houses.

Karlsson and Huber (1996) summarized the sorption/desorption model parameters, a and b , for Cl_2 based on an earlier experimental study. The experimental setup was a 38 [m³] room with painted walls, roof, and flat plastic carpet. The total surface area was 79 [m²]. The test conditions were as follows: 15-20 °C, <50% RH, 0.14-0.25 ACH, and initial concentration of 37-51 [mg/m³]. Results from two trials suggested that $a = 1.4(\pm 0.6) \cdot 10^{-4}$ [m/s] and $b = 0.033 \pm$

0.012 [m⁻¹]. These parameters are assumed to apply for all indoor surfaces.

By dividing Eqn. (4) with volume of the dwelling V [m³], the mass balance becomes

$$\frac{dC}{dt} = \frac{Q_f}{V} \cdot (C_{out} - C) - \frac{A_s}{V} \cdot \frac{dm}{dt} \quad (9)$$

where A_s/V [m⁻¹] is the indoor surface area to volume ratio. Indoor surface area includes not only the walls, floor, and ceiling, but also some additional surfaces for furnishings. The parameter is not well studied, but it is thought to be in the range of 2 to 4 [m⁻¹] (Knutson, 1988). Q_f/V [s⁻¹] can be calculated by substituting Eqn. (7) into (1):

$$\frac{Q_f}{V} = \frac{\sqrt{f_s^2 \cdot |\Delta T| + f_w^2 \cdot v^2}}{1000} \cdot \frac{NL}{H} \cdot \left(\frac{2.5[m]}{H} \right)^{0.3} \quad (10)$$

In the discussion to follow, we only show results for the 50th percentile NL of each Census tract (see Fig. (1)). Further, we assumed the heights of dwellings are deterministic at 3 [m], 5.5 [m], and 8 [m] for 1, 2, and 3-story dwellings respectively, and that NL is not a function of height. The nationwide proportions of 1, 2, and 3-story dwellings are approximately 66%, 32%, and 2% based on the American Housing Survey (1999). The model is solved separately for 1, 2, and 3-story dwellings, and the weighted-average indoor concentrations are reported as the model results.

3.4 Model Results

Indoor concentration predictions are displayed in Fig. (4) (see Appendix). Compared to the outdoor predictions, the concentrations indoors are much lower. The indoor concentrations also appear over a larger area than the outdoor plume. This is partly because the outdoor plume meandered considerably. Some pockets of contaminants only appeared for a short duration and were not captured by the snapshots of the concentration field shown in Fig. (4). More importantly, contaminants exfiltrate from the indoors slowly as governed by the air exchange rate. When the plume passed by an area, some contaminants entered the houses and did not get flushed out for many

typically follow visible features such as roads, rivers, canals, railroads, etc.

hours. Therefore the indoor concentration maps essentially captured the time history of the plume pathway. The effect of sorption/desorption is also evident from the slightly lighter shading, representing lower concentrations, compared to the no sorption case.

To illustrate the relative importance of sorption/desorption to the effectiveness of shelter-in-place, Fig (2) shows the concentration profiles predicted for a dwelling of typical leakiness (50th percentile NL). This dwelling is located approximately 10 [km] downwind from the release source. The outdoor concentration profile shows some meandering of the Cl₂ plume. The remaining profiles are indoor predictions. Even without considering the sorption/desorption process, the indoor peak concentration is more than an order of magnitude lower than outdoor. When sorption/desorption effects are taken into account, the indoor concentration predictions are reduced by an additional 50%.

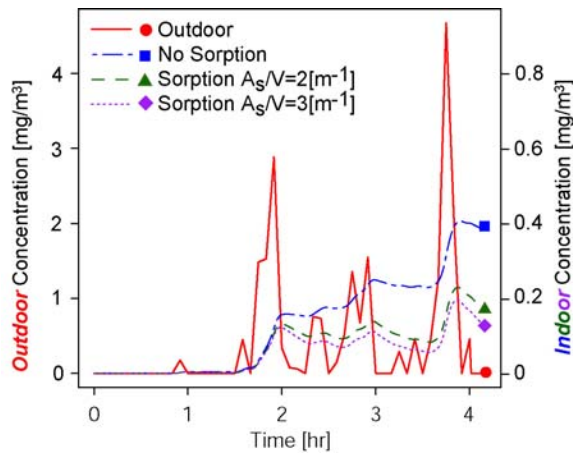


Fig. (2) Concentration profiles of a typical dwelling located 10 [km] downwind of the release source.

The sensitivity of the model to A_s/V is only moderate. However, since the confidence regarding the typical range of A_s/V is low, it is possible that the overall uncertainty of this term is significant. Further, only limited types of surfaces were used in the experiments from which sorption/desorption parameters are derived. The variability in the quality and quantity of the surfaces are both important but they are not well studied. These uncertainties

require more in-depth sensitivity analysis to quantify.

One measure of the overall effect of shelter-in-place is the total intake of the population. Total population intake I [g] is defined as:

$$I = \int_{time} \int_{grid} \frac{C}{10^3} \cdot BR \cdot \rho_{pop} d(grid) d(time) \quad (11)$$

where C [mg/m^3] is the concentration, BR [m^3/s -person] is the breathing rate, and ρ_{pop} [$persons/m^2$] is the population density. Census tract level population density is obtained from the 2000 Census survey. Breathing rate is a function of gender, age, and activity level. The gender and age of the population in Albuquerque are obtained similarly from the 2000 Census survey. Assuming a light activity level, BR is computed according to the recommendations of the EPA Exposure Factors Handbook (1997). The values of BR range from 0.66 to 0.78 [m^3/h] in the 26 census tracts exposed to the simulated Cl_2 plume. The estimated intakes are shown in Fig. (3).

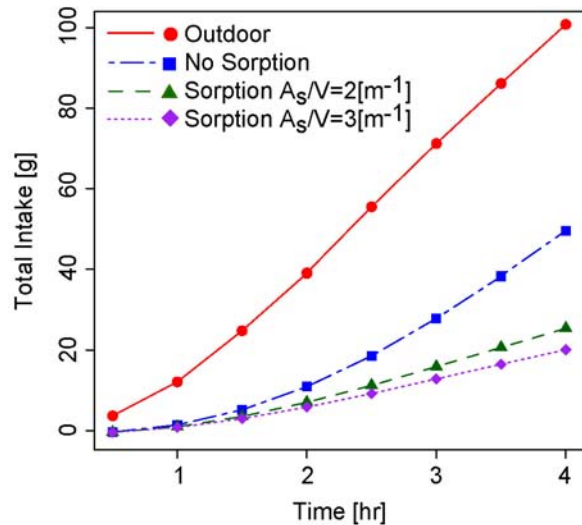


Fig. (3) Estimated total population intake as defined in Eqn. (11).

By sheltering indoors, the total population intake at the end of a 4-hour release for a non-sorbing gas is approximately 50% less than the outdoor value. The reduction is even more profound when sorption/desorption is taken into account. Total intake of the population at the

end of the 4-hour release is about half of the no-sorption case. These ratios are expected to change if we were to extend the simulation for longer period of time. Once the outdoor plume has blown out of the model domain, the total intake from outdoor exposures will level off. At approximately the same time, SIP should be terminated and people should leave the buildings so as to minimize their exposures. These events are not modeled here but they are important aspects of a successful SIP strategy. Furthermore, the results shown here are specific to Cl₂ only. The effect of sorption/desorption can be more or less important depending on the properties of the substance and the type and amount of indoor surfaces presented.

4. CONCLUSION

We have presented a case study of simulated SIP during a hypothetical Cl₂ release simulated by NARAC. We used the LBL infiltration model to calculate the distribution of infiltration rates within each Census tract. A simple treatment of sorption/desorption shows that the process adds another level of protection to occupants during SIP.

Total population intake is used in our analysis as the metric of comparison. We expect the benefit of SIP to be greater if we were to consider the non-linear dose-response curve of Cl₂. Like many toxic industrial substances and chemical warfare agents, avoiding exposure to peak concentration is a worthwhile trade-off for longer exposure at a lower concentration. Buildings acting as low-pass filters provide exactly this type of desirable protection. Sorption to surfaces further lowers the peak concentration and therefore enhances the effectiveness of SIP.

A number of implications are evident from this case study. First, there is a large variability in the air tightness among residential buildings that needs to be addressed when assessing the effectiveness of SIP. Second, the uncertainty of this analysis is expected to be quite large owing to the limited sorption/desorption data. More experimental studies on sorption/desorption of various industrial toxic substances and surrogates of chemical warfare agents are needed. Finally, the importance of prompt termination of SIP is not discussed here but the method outlined can be part of a real-time

decision analysis system capable of advising emergency response strategies.

5. ACKNOWLEDGEMENT

The authors would like to thank Rob Harley and Rich Corsi for their advices, and Brett Singer and Buvanewari Jayaraman for their reviews.

This work was supported by the Office of Chemical Biological Countermeasures, of the Science and Technology Directorate of the Department of Homeland Security, and performed under U.S. Department of Energy Contract No. DE-AC03-76SF00098. Work done at NARAC was performed under the auspices of the U.S. Department of Energy by the University of California, Lawrence Livermore National Laboratory under contract No. W-7405-Eng-48.

6. REFERENCE

- American Housing Survey National Data, 1999: <http://www.census.gov/hhes/www/housing/ahs/nationaldata.html>.
- Blewett WK, Reeves DW, Arca VJ, Fatkin DP, Cannon BD, 1996: Expedient sheltering in place: an evaluation for the chemical stockpile emergency preparedness program, Chemical Research, Development & Engineering Center, ERDEC-TR-336, Aberdeen Proving Ground.
- Blewett WK, Arca VJ, 1999: Experiments in sheltering in place: how filtering affects protection against sarin and mustard vapor, Edgewood Chemical Biological Center, ECBC-TR-034, Aberdeen Proving Ground.
- Chan WR, Price PN, Sohn MD, Gadgil AJ, 2003: Analysis of US residential air leakage database, Lawrence Berkeley National Laboratory, LBNL 53367, Berkeley.
- EPA Exposure Factor Handbook, 1997: 1(5), Inhalation Route, Washington DC.
- Karlsson E, Huber U, 1996: Influence of desorption on the indoor concentration of toxic gases, *Journal of Hazardous Materials*, **49**, 15-27.

Knutson EO, 1988: Modeling indoor concentrations of radon's decay products, WW Nazaroff, AV Nero, Eds., *Radon and Its Decay Products in Indoor Air*, John Wiley & Sons, New York.

Manna MS, Kilpatrick DL, 2000: The pros and cons of shelter-in-place, *Process Safety Process*, **19** (4), 210-218.

Nazaroff WW, Alvarez-Cohen L, 2001: Environmental Engineering Science, Ch 3, John Wiley & Sons, New York.

Sherman MH, 1980: Air Infiltration in Buildings, PhD Thesis, University of California, Berkeley.

Sorensen JH, Vogt BM, 2001: Will duct tape and plastic really work? Issues related to expedient shelter-in-place, Oak Ridge National Laboratory, ORNL/TM-2001/154, Oak Ridge.

Vogt BM, Hardee HK, Sorensen JH, Shumpert BL, 1999: Assessment of housing stock age in the vicinity of chemical stockpile sites, Oak Ridge National Laboratory, ORNL TM-13742, Oak Ridge.

7. APPENDIX

Table 1. Terrain parameters for LBNL infiltration model.

Terrain Class	Terrain Description	A	B
I	Ocean / Water body	1.30	0.10
II	Flat with some isolated obstacles	1.00	0.15
III	Rural areas	0.85	0.20
IV	Urban, industrial, forest areas	0.67	0.25
V	Large city center	0.47	0.35

Table 2. Shielding parameters for LBNL infiltration model.

Terrain Class	Terrain Description	C
I	No obstructions	0.34
II	Light local shielding	0.30
III	Some obstructions	0.25
IV	Obstructions around most of perimeter	0.19
V	Large obstructions surrounding perimeter	0.11

Table 3. Multi-variable linear regression parameters for the normalized leakage of low-income and conventional single-family detached dwellings.

Parameters Estimates*	Low-Income Dwellings	Conventional Dwellings
β_0	$1.11 \cdot 10^1$	$2.07 \cdot 10^1$
β_1	$-5.37 \cdot 10^{-3}$	$-1.07 \cdot 10^{-2}$
β_2 [m ⁻²]	$-4.18 \cdot 10^{-3}$	$-2.20 \cdot 10^{-3}$

* Standard errors and t-values for these parameters are tabulated in Chan et al. (2003).

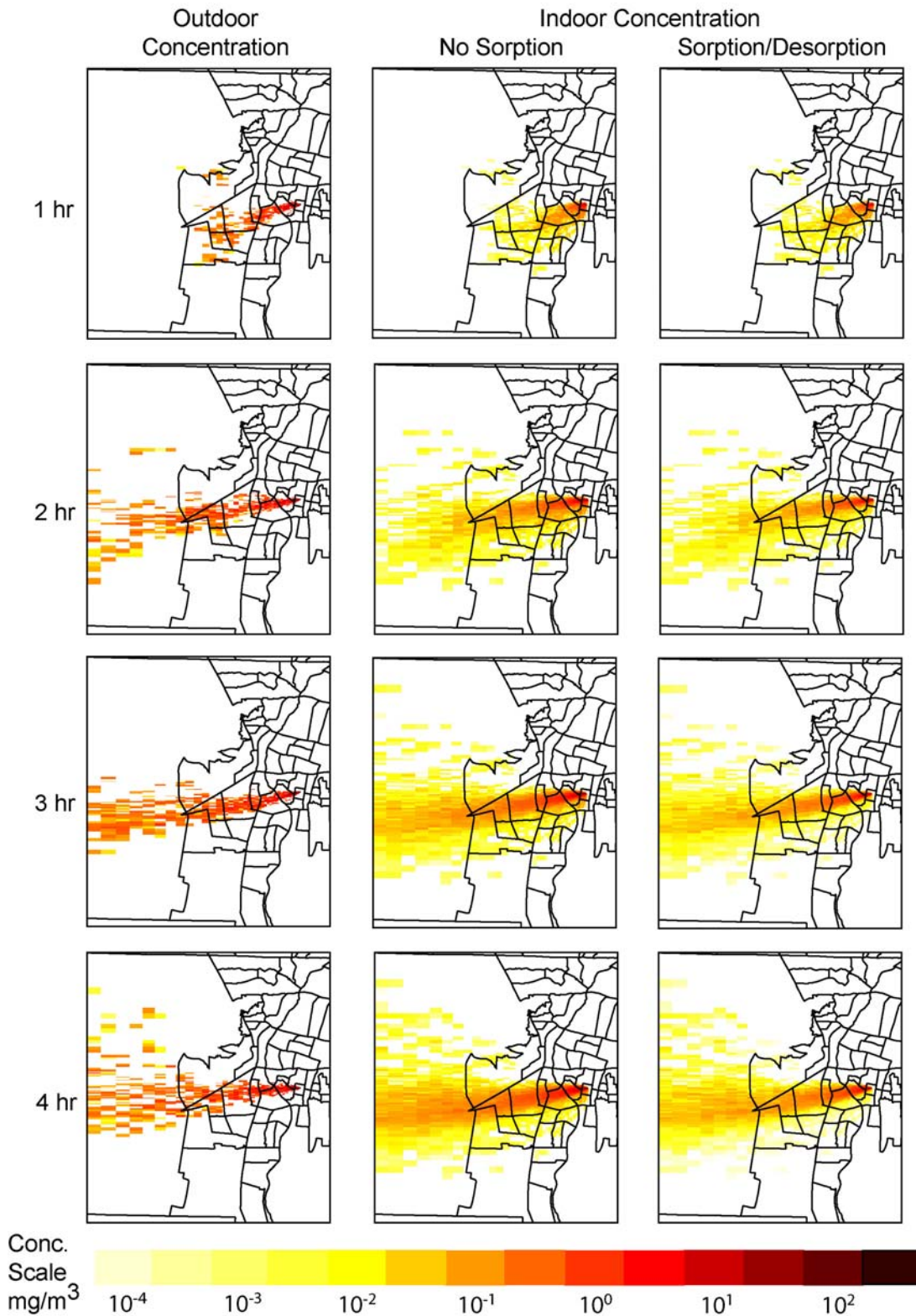


Fig. (4) 15-minute time-averaged concentration maps (27 x 30 [km]) of outdoor and indoor environments with and without sorption ($A_s/V=2[\text{m}^{-1}]$). The geographical features shown are census tracts. Times are referenced to onset of release.